

Comparison of cracking behavior of nanocrystalline Cu film on substrates of different plastic deformation mechanisms

G. Zhang ^a, T. Wang ^{a,b}, Z. Ma ^a, H. Zhou ^c, L. Cui ^a, K.Y. Yu ^{a*}

^a Department of Materials Science and Engineering, China University of Petroleum-Beijing, Beijing 102249, China

^b School of Materials Science and Engineering, Shaanxi University of Technology, Hanzhong, Shaanxi 723001, China

^c X-ray Science Division, Argonne National Laboratory, Lemont, IL 60439, USA

Abstract

Nanocrystalline (NC) metallic thin films on metal substrates usually undergo substantial cracking at applied strains of a few percent due to strain concentration at the film/substrate interfaces. In this work, we show that the cracking of a nanocrystalline Cu film can be significantly inhibited by a NiTi alloy substrate. NC Cu films are deposited on 304 stainless steel, Kapton and NiTi substrates, in which plastic deformation occurs via dislocation slip, molecule chain disentanglement and collective lattice shear, respectively. NC Cu film on NiTi substrate starts to show observable cracks at an applied strain of 24%, in contrast to 6% for that on steel and 15% for that on Kapton. The crack density in the film on NiTi is two to three orders lower than the counterparts. The discrepancy is suggested to attribute to the reduced local strain concentration enabled by the uniform lattice shear and high strain hardening of NiTi substrate.

Keywords: nanocrystalline, thin film, ductility, crack, martensitic transformation, NiTi

Corresponding author: K.Y.Yu kyyu@cup.edu.cn

1. Introduction

Nanostructured metallic thin films are promising candidates for a large variety of applications due to the superior combination of structural and functional properties to their counterparts [1-6]. In the past decades, extensive efforts have been dedicated to the understanding of the deformation behaviors of nanostructured metallic thin films in order to improve their durability or stability during service [7-11]. While exceptional properties such as high strength, hardness and wear resistance have been well-established, the achievement of reasonable ductility remains a major challenge in order to reduce the risk of early cracking of the films [8, 9, 12-15].

Freestanding nanostructured metallic films are known to crack significantly at small strains typically less than a few percent, due to their limited work hardening capacity and the great length-to-thickness ratio [16-18]. When the films are deposited onto ductile substrates, the cracking is to some extent inhibited due to the strong constraint effect between the films and substrates to suppress the strain localization in the films [19, 20]. One typical type of the ductile substrates is polymers. Polymer substrates undergo plastic deformation through molecule chain disentanglement in a relative uniform manner without introducing structural defects [21, 22]. In this regard, the strain concentration associated with the structural defects is limited at the film/substrate interface such that the ductility of the films can be mostly retained. For instance, Cu films of 1 μm in thickness on Kapton substrates (with Cr as an adhesion layer) can be stretched up to 50% before cracking [23]. However, as the thicknesses or grain sizes approach the nanoscale (<100 nm), the thin films are difficult to deform plastically because of dimensional constraints on dislocation activity [24, 25]. In this case, the high level of stress triggers grain boundary decohesion or film delamination before ductility occurs and the total elongation at failure is typically small [24].

A second type of the ductile substrates is metals that deform by dislocation slip. It has been shown that the ductility of a nanocrystalline (NC) Ni thin film can be enhanced by a coarse-grained (CG) Cu substrate, owing to the suppression of strain localization from the CG Cu substrate [26]. Such a wisdom has been widely applied in nanostructured bulk metals by creating bimodal [27], heterogeneous [28] and gradient structures [29]. These strategies all allow well-accommodated plastic

deformation between the constituents. But in a film/substrate system, the suppression of the strain localization from the substrate is usually not sufficient. Upon the yielding of the metallic substrate, a high density of dislocations pile up at the film/substrate interfaces, leading to a significant increase in the strain concentration. To accommodate the plastic strain of the substrate, shear banding in the thin film often occurs at a small strain and results in early rupture of the film [26, 30].

According to the above analyses, two requirements for the selection of substrates can be inferred. First, the plastic deformation of the substrates should introduce as few structural defects (*e.g.* dislocations) as possible to mitigate the strain concentration at the film/substrate interfaces. Second, the adhesion between the films and substrates should be strong in order to suppress the delamination or necking of the films. We suggest that the two requirements may be met by using NiTi shape memory alloys (SMAs) as substrates. NiTi SMAs undergo stress-induced martensitic transformation (SIMT) during deformation [31, 32]. The transformation strain is generated by collective lattice shear, which is uniform and essentially different from the deformation mechanism based on dislocation slip in conventional metals [32-37]. Such a characteristic of NiTi is effective in relieving the strain concentration and has allowed the neighboring constituents to exhibit ultra large elastic strain limit in a large variety of composite systems [32-37]. Most recently, similar results have been justified in a Nb/NiTi film/substrate system [38]. Despite that the previous studies have mostly concentrated on the elastic deformation of the films (or the neighboring constituents), they all suggest that the unique deformation behavior of NiTi strongly affects the deformation behavior of its neighbors. In this sense, the cracking behavior of a thin film on a NiTi substrate may be significantly different from that on other substrates. It is possible that the early cracking of a nanocrystalline thin film may be inhibited by the NiTi substrate. In addition, compared to polymer substrates, NiTi have much better adhesion to metal films. As such, the prefabrication of a transition metal layer is probably unnecessary and hence the risk of early cracking associated with transition layer can be reduced [23].

In this study, we fabricated NC Cu films on three different substrates, *i.e.* the steel substrate, Kapton substrate and NiTi substrate. The deformation and cracking

behaviors of the NC Cu films were examined and compared. The onset strain of cracking and crack density were measured for each specimen to characterize the cracking behavior. The plastic deformation mechanism of NC Cu film on NiTi substrate was investigated by atomic force microscopy (AFM).

2. Material and Methods

Commercial 304 stainless steel (0.3 mm in thickness), Kapton (0.1 mm in thickness) and NiTi (0.3 mm in thickness) plates were used to fabricate the substrates used in this study. The atomic composition of the NiTi plate was Ni50.7-Ti49.3. It was obtained by cold-rolling a thicker plate (0.6 mm in thickness, solution-treated at 700 °C and water-quenched) to a thickness reduction of 50%. The as-rolled plate was then annealed at 400 °C for 30 min. The as-annealed plate has a martensitic transformation starting temperature (M_s) of -10 °C and an R -phase starting temperature (R_s) of 20 °C (Fig. S1). The NiTi substrates used in this study were consisted of single B2 phase as the experiments were performed at room temperature (~25 °C).

The three types of plates were cut into dog-bone shaped substrates with a gauge length of 20 mm. Steel and NiTi substrates were subjected to mechanical polishing to mirror level. All substrates were ultrasonically cleaned by acetone and ethanol and blown by nitrogen gas before being placed into the sputtering chamber. The base pressure of the chamber was 1.0×10^{-7} Torr. The purity of the Cu target was 99.995 at. %. Cu films of 50 nm in thickness were deposited onto the gauge area of the substrates with a DC power of 200 W and a working gas (Ar) pressure of 3.2×10^{-3} Torr using a K.J. Lesker Labline sputtering system. The target-to-substrate distance was 100 mm and the deposition rate was 0.39 nm s^{-1} . The sample stage was rotating at a speed of 5 r/min during deposition. As-deposited specimens were kept in vacuum before testing to avoid possible oxidation and contamination. Tensile tests were formed using a WDT II-20 Instron-type tensile machine at a strain rate of $5 \times 10^{-4} \text{ s}^{-1}$. During tensile tests, the electrical resistance of the specimens was measured using a Keithley 2000 four-point probe system. Thermally-induced transformation of the NiTi substrate was examined using a Q20 differential scanning calorimeter (DSC) at a cooling and heating rate of 5 K/min. The microstructure of the films was

characterized using an FEI Tecnai F20 transmission electron microscope (TEM). The film surface morphology before and after tensile tests was characterized using a Quanta 200 scanning electron microscope (SEM) and an Agilent 5500 atomic force microscope (AFM).

3. Results and discussion

Fig. 1a is a bright-field TEM image of NC Cu film deposited on carbon-coated TEM washer, showing equiaxed nanosized grains. The inset is a selected-area electron diffraction (SAD) pattern showing the face-centered-cubic crystal structure of the film. The average grain size is about 31 nm based on the TEM image, as shown in Fig. 1b. Fig. 1c shows an AFM image of NC Cu film deposited on NiTi substrate. Equiaxed nanosized grains were observed on the surface of the film. Fig. 1d shows that the average grain size is about 30 nm, which is consistent with that in Fig. 1b. The grain size of NC Cu films on the steel substrate is about 32 nm as shown in Fig. S2a-b, and that on Kapton substrate is about 11 nm as shown in Fig. S5c-d. The difference in the grain size is probably related to the different wetting and diffusion properties of the film (during nucleation stage) on metal and polymer substrates.

Uniaxial tensile tests were carried out to examine the cracking behavior of the NC Cu films on different substrates at different strains. The morphological change of the NC Cu films were examined by SEM and the results are shown in Fig.2. For NC Cu films on steel substrate at the strain of 6% (Fig. 2 a), very few cracks were observed. Deformation bands along 45° with respect to the loading direction (the horizontal direction) were present. The formation of these deformation bands is due to the formation of the deformation bands on the surface of the steel substrate [39] . At the strain of 24% (Fig. 2b), a high density of cracks appeared in the NC Cu film probably due to the strain mismatch between the substrate and the film. Moreover, film delamination was observed at the areas where cracks of different propagation directions crossed, as labeled by the arrows in Fig. 2b. These areas seem corresponding to the grain boundaries of the steel substrates. The grain boundaries were presumed as where the fronts of the deformation bands of different orientations encountered. As a possible result, large strain was concentrated at these areas and hence film delamination occurred. The enlarged view in Fig. 3a shows that the cracks

were long and straight in shape and crossed the whole steel grain. This implies that the crack propagation was barely mitigated by the steel substrate.

In comparison, the crack morphology of NC Cu films on Kapton substrate was very different. At 6% strain (Fig.2c), no cracks or any other morphological changes were observed. The film was nearly intact. At 24% strain (Fig.2d), cracks perpendicular to the loading direction were observed. In contrast to those in the NC Cu film on steel substrates, the cracks here were short and zigzag in shape, as shown by the enlarged image in Fig. 3b. This is because the plastic deformation of the film was confined by the uniform elongation of Kapton substrate, as previously reported [24]. Moreover, the strain hardening of Kapton substrate may have hindered the crack propagation, resulting in the zigzag shape of cracks.

Figs. 2e-f show the morphology of NC Cu film deposited on NiTi substrates subjected to different strains. At the strain of 6%, the film was nearly intact. When the strain reached 24%, deformation bands appeared on the surface of the NC Cu film, similar to those in film on steel substrate at 6% (Fig.2a). Slight deformation bands were observed occasionally at lower strain (9%-12%). A close examination shows only one crack over the entire film surface, as shown in Fig.3c. More SEM images are shown in Fig. S3. Fig. 4 compares the crack density in NC Cu films on different substrates, as a function of strain. The crack density was defined as the crack length per unit area. With increasing strain, the crack density of NC Cu film on steel substrate increased rapidly from 3% to 9% of strain and became nearly saturated after the strain of 12%. The maximum crack density was about $8 \mu\text{m}/\mu\text{m}^2$ at the strain of 26%. In comparison, the crack density of Cu films on Kapton substrate was about two orders lower. The maximum crack density was about $1.3 \times 10^{-1} \mu\text{m}/\mu\text{m}^2$ at the strain of 26%. From 0% to 15% of strain, the cracks were not observed. An abrupt increase of crack density was observed when the strain exceeds 24%. Last, the crack density of NC Cu film on NiTi substrate was the lowest. The cracks were not observed from 0% to 24% of strain. At the strain of 26%, the crack density was only $9 \times 10^{-3} \mu\text{m}/\mu\text{m}^2$. These results suggest that the NiTi substrate can inhibit the crack growth and propagation in the NC Cu film more effectively than the steel and Kapton substrate.

It must be noted that the onset cracking strains measured by SEM could be upper

bound values since non-detectable microcracks may be present way earlier. A more precise method to characterize the onset cracking could be measuring the electrical resistance (R) of the films during tension [23-25, 40] because R is very sensitive to the structural variation of the films. It has been shown that the onset strain of cracking can be determined by the deviation of R from linearity with increasing strain (R increases abruptly upon cracking) [23, 24]. Our results in Fig. S4a-b show consistent results to literature. However, such a method is not applicable for films on NiTi substrates. This is because the NiTi substrate underwent SIMT during which R changes significantly [32, 41] and hence the R variation of the film is difficult to examine. As shown in Fig. S4c, $\Delta R/R_0$ of NC Cu film on NiTi substrate first increased linearly with increasing strain and then deviated downwards with respect to the initial linear stage. This is in sharp contrast to the upward deviation in literature [23, 24]. For this reason, such a method cannot be used to characterize the cracking behavior of the NC Cu film on NiTi substrate. The SEM-based results (Fig. 4), although probably not accurate in this sense, are sufficiently useful in terms of making fair comparison between the cracking behaviors of the films on different substrates.

We next discuss the possible mechanism of the inhibited cracking of NC Cu film on NiTi substrate. Fig. 5 depicts the stress-strain curves and the deformation mechanisms of the three substrates. For the steel substrate, apparent yielding was observed below the strain of 1% (Fig. 5a). This is probably the point when massive dislocation activities occurred. Meanwhile, a high density of dislocations may pile up against the film/substrate interface, leading to high strain concentration and hence local cracking. Since only limited preferential slip systems in a specific grain of the substrate operated at the early stage of plastic deformation, the strain concentration could not be mitigated instantaneously by strain hardening. As a result, the cracks, once formed, propagated rapidly along the deformation bands in a straight manner over a long distance (Fig.3a). In contrast, Kapton substrate deformed via the molecule chain disentanglement, during which no structural defects like dislocations were introduced (Fig. 5b). Therefore, the strain concentration at the film/substrate interface was minor. This is the reason that its onset strain of cracking was much larger (Fig.4). By comparison, the NiTi substrate deformed successively by B2 \rightarrow B19' SIMT (the

plateau regime), combined elastic and plastic deformation of B19' martensite (the hardening regime) and plastic deformation of B19' martensite, as shown in Fig. 5c. During the first two regimes, limited structural defects were introduced at the film/substrate interface [34-36, 42]. The uniform lattice shear of SIMT prevented high local strain concentration and assured a relatively uniform strain distribution at the interface [34-36, 42], thus preventing the premature failure of the film. After that, the B19' martensite rapidly stiffened with increasing strain due to dislocation and variant interactions [43-46], which may further inhibit the crack propagation in the films.

We last examine the deformation behavior of NC Cu film on NiTi substrate before cracking. It is well-known that dislocation activities are largely inhibited at such a small grain size (30 nm) [4]. It therefore remains unclear microscopically what has carried the plastic deformation of NC Cu films before cracking. Due to the difficulty in obtaining TEM specimens for such thin films that are strongly bonded to substrates, we observed the morphological variation of NC Cu films by AFM. Fig. 6 shows the AFM results of NC Cu film on NiTi substrate at different strains. Prior to deformation, the grains were equiaxed in shape and the average grain size was about 30 nm, as shown in Figs. 6a-b. At the strain of 12%, the grains remained equiaxed but the average grain size increased to 50 nm (Figs. 6c-d). When the strain reached 21%, some of the grains appeared elongated along the shear direction ($\approx 45^\circ$), as outlined by the dash lines in Fig. 6e. Furthermore, the average grain size increased to 187 nm as seen in Fig. 6f. More AFM images can be found in Fig. S5. These results indicate that the plasticity of the NC Cu films was significantly mediated by dynamic grain growth in addition to dislocation activities. In contrast, significant dynamic grain growth was not observed in Cu films on steel and Kapton substrate (Fig. S6 and S7).

The grain boundary mediated plasticity has been observed in a large variety of NC metals such as the NC Al foil under *in situ* compression and the NC Cu surface layer in a gradient structure under tension [29, 47-53]. It has been suggested that the dynamic grain growth is mechanically driven (or stress-assisted) and could be attributed to defect annihilation in nanograins in order to reduce the excessive grain boundary energy [4, 29, 47]. A full understanding of grain boundary mobility and grain growth is not available to date [4]. In case of our NC Cu on NiTi substrate, the

grain growth may be triggered by two factors. First, SIMT of NiTi may have inhibited the possible failure associated with grain boundary shearing. Simulation results in NC Ni have suggested that deformation mechanism becomes grain-boundary shearing or sliding when the average grain size decreases down to 10 nm [54, 55]. It is possible that SIMT reduces the local stress caused by grain-boundary shearing or sliding and thus favors the dynamic grain growth process. Second, there is a possibility that the heat released during SIMT may have increased the local temperature of the film [56, 57]. As such, the grain growth is thermally triggered. As for the absence of dynamic grain growth in NC Cu film on steel and Kapton substrates, it is probably a result of the competition of grain growth and cracking. These two mechanisms both tend to release the localized strain energy in the film. As shown in Fig. 4, the cracking in Cu films on steel and Kapton occurs much earlier than that on NiTi. As a result, the strain energy has been released by cracking such that the grain growth cannot be mechanically driven. These postulated mechanisms were not the focus of the present study but may be confirmed in the future by using *in situ* techniques. But the dynamic grain growth observed at least implies that the plastic deformation behavior of NC Cu films on NiTi substrate may be rate-dependent [4, 52, 53]. In this sense, their cracking behavior, which is tightly related with plastic deformation, may also be rate-dependent. Different cracking behavior (or enhanced cracking tolerance) may thereby be expected by changing the strain rate (Fig. S8). The onset cracking strain of NC Cu film increased with decreasing strain rate. Lower strain rates allow the grain boundary mediated plasticity to better accommodate the applied strain. As a result, the strain localization is delayed and hence the onset strain of cracking is enhanced.

4. Conclusion

NC Cu films were sputter-deposited on steel, Kapton and NiTi substrates. The deformation and cracking behaviors of the films were investigated and compared. The onset strain of cracking in NC Cu film on NiTi substrate was 24%, in contrast to 6% for film on steel and 15% for film on Kapton. Before evident cracking, NC Cu film undergoes plastic deformation during which the average grain size increased from 30 nm to 180 nm. It was suggested that the inhibited cracking of NC Cu film on NiTi

substrate was probably attributed to the uniform lattice shear of SIMT and the high strain hardening rate of B19' martensite.

Acknowledgement

K.Y. acknowledges financial supports from National Natural Science Foundation of China (NSFC 91963112 and 51871241). L.C. acknowledges financial supports from National Natural Science Foundation of China (NSFC 51731010 and 51971243).

References

- [1] J.A. Rogers, Electronics. Toward paperlike displays, *Science* 291 (2001) 1502-1503.
- [2] Y. Liu, M. Pharr, G.A. Salvatore, A Lab-on-Skin: A Review of Flexible and Stretchable Electronics for Wearable Health Monitoring, *ACS Nano* 11 (2017) 9614-9635.
- [3] T. Carey, S. Cacovich, G. Divitini, J. Ren, A. Mansouri, J.M. Kim, C. Wang, C. Ducati, R. Sordan, F. Torrisi, Fully inkjet-printed two-dimensional material field-effect heterojunctions for wearable and textile electronics, *Nat Commun.* 8 (2017) 1202.
- [4] M. Dao, L. Lu, R.J. Asaro, Toward a quantitative understanding of mechanical behavior of nanocrystalline metals, *Acta Mater.* 55 (2007) 4041-4065.
- [5] Y. Hu, G. Yang, Z. Tian, Z. Hu, Effect of annealing on the structural and thermoelectric properties of nanostructured Sb₂Te₃/Au semiconductor/metal multilayer films, *J. Alloy. Compd.* 790 (2019) 723-731.
- [6] K. Higuchi, K. Yamamoto, H. Kajioaka, K. Toiyama, M. Honda, S. Orimo, H. Fujii, Remarkable hydrogen storage properties in three-layered Pd/Mg/Pd thin films, *J. Alloy. Compd.* 330-332 (2002) 526-530.
- [7] A. Misra, J.P. Hirth, R.G. Hoagland, Length-scale-dependent deformation mechanisms in incoherent metallic multilayered composites, *Acta Mater.* 53 (2005) 4817-4824.
- [8] J. Wang, A. Misra, An overview of interface-dominated deformation mechanisms in metallic multilayers, *Curr. Opin. Solid State Mater. Sci.* 15 (2011) 20-28.
- [9] J.Y. Zhang, S. Lei, J. Niu, Y.Liu, G. Liu, X. Zhang, J. Sun, Intrinsic and extrinsic size effects on deformation in nanolayered Cu/Zr micropillars: From bulk-like to small-volume materials behavior, *Acta Mater.* 60 (2012) 4054-4064.
- [10] J. Shu, R. Yang, Y. Chang, X.Q. Guo, X. Yang, A flexible metal thin film strain sensor with micro/nano structure for large deformation and high sensitivity strain measurement, *J. Alloy. Compd.* 879 (2021) 160466.
- [11] Q. Zhou, Y. Ren, Y. Du, D.P. Hua, W.C. Han, Q.S. Xia, Adhesion energy and related plastic deformation mechanism of Cu/Ru nanostructured multilayer film, *J. Alloy. Compd.* 772 (2019) 823-827.
- [12] A. Pineau, A. Amine Benzerga, T. Pardoen, Failure of metals III: Fracture and fatigue of nanostructured metallic materials, *Acta Mater.* 107 (2016) 508-544.
- [13] N. Lu, S. Yang, Mechanics for stretchable sensors, *Curr. Opin. Solid State Mater. Sci.* 19 (2015) 149-159.
- [14] J.A. Rogers, T. Someya, Y. Huang, Materials and Mechanics for Stretchable Electronics, *Science* 327 (2010) 1603-1607.
- [15] Y. Wang, J. Li, A.V. Hamza, T.W. Barbee, Ductile crystalline-amorphous nanolaminates, *PNAS* 104. 27 (2007) 11155-11160.
- [16] R.R. Keller, J.M. Phelps, D.T. Read, Tensile and fracture behavior of free-standing copper films, *Mater. Sci. Eng. A* 214 (1996) 42-52.
- [17] R.D. Emery, D.X. Lenshek, B. Behin, M. Gherasimova, G.L. Povrik, Tensile Behavior of Free-Standing Gold Films, *Mrs Proc.* 472.472 (1997) 361.
- [18] M.A. Haque, M.T. A Saif, Mechanical behavior of 30–50 nm thick aluminum films under uniaxial tension, *Scripta Mater.* 47 (2002) 863-867.

- [19] T. Li, Z. Suo, Ductility of thin metal films on polymer substrates modulated by interfacial adhesion, *Int. J. Solids. Struct.* 44 (2007) 1696-1705.
- [20] X. Yong, T. Li, Z. Suo, J.J. Vlassak, High ductility of a metal film adherent on a polymer substrate, *Appl. Phys. Lett.* 87 (2005) 161910.
- [21] B.L. Smith, T.E. Schaeffer, M. Viani, J.B. Thompson, N.A. Frederick, J. Kindt, Molecular mechanistic origin of the toughness of natural adhesives, fibres and composites, *Nature* 399 (1999) 761-763.
- [22] P.Y. Chen, J. McKittrick, M.A. Meyers, Biological materials: Functional adaptations and bioinspired designs, *Prog. Mater. Sci.* 57 (2012) 1492-1704.
- [23] N. Lu, X. Wang, Z. Suo, J.J. Vlassak, Metal films on polymer substrates stretched beyond 50%, *Appl. Phys. Lett.* 91 (2007) 221909.
- [24] N. Lu, Z. Suo, J.J. Vlassak, The effect of film thickness on the failure strain of polymer-supported metal films, *Acta Mater.* 58 (2010) 1679-1687.
- [25] R.M. Niu, G. Liu, C. Wang, G. Zhang, X.D. Ding, J. Sun, Thickness dependent critical strain in submicron Cu films adherent to polymer substrate, *Appl. Phys. Lett.* 90 (2007) 161907.
- [26] D. Qi, J. Zhou, H. Liu, S. Dong, Y. Wang, Strain-delocalizing effect of a metal substrate on nanocrystalline Ni film, *Mater. Sci. Eng. A* 640 (2015) 408-418.
- [27] Y. Wang, M. Chen, F. Zhou, E. Ma, High tensile ductility in a nanostructured metal, *Nature* 419 (2002) 912-915.
- [28] X. Wu, Y. Zhu, Heterogeneous materials: a new class of materials with unprecedented mechanical properties, *Mater. Res. Lett.* 5 (2017) 527-532.
- [29] T.H. Fang, W.L. Li, N.R. Tao, K. Lu, Revealing Extraordinary Intrinsic Tensile Plasticity in Gradient Nano-Grained Copper, *Science* 331 (2011) 1587-1590.
- [30] B.Q. Yang, K. Zhang, G.N. Chen, G.X. Luo, J.H. Xiao, Measurement of fracture toughness and interfacial shear strength of hard and brittle Cr coating on ductile steel substrate, *Surf. Eng.* 24 (2013) 332-336.
- [31] S. Miyazaki, K. Otsuka, Y. Suzuki, Deformation and transition behavior associated with the R-phase in Ti-Ni alloys, *Metall. Trans. A* 17.1 (1986) 53-63.
- [32] K. Otsuka, X. Ren, Physical metallurgy of Ti-Ni-based shape memory alloys, *Prog. Mater. Sci.* 50 (2005) 511-678.
- [33] Z. Chen, Z. Ma, K.Y. Yu, T. Wang, E.G. Fu, G. Zhang, L. Cui, Strengthening mechanisms in NiTi(NbFe)/amorphous-CuZrAl multilayered thin films, *Surf. Coat. Tech.* 353 (2018) 247-253.
- [34] S. Hao, L. Cui, D. Jiang, X. Han, Y. Ren, J. Jiang, Y. Liu, Z. Liu, S. Mao, Y. Wang, Y. Li, X. Ren, X. Ding, S. Wang, C. Yu, X. Shi, M. Du, F. Yang, Y. Zheng, Z. Zhang, X. Li, D.E. Brown, J. Li, A Transforming Metal Nanocomposite with Large Elastic Strain, Low Modulus, and High Strength, *Science* 339 (2013) 1191-1194.
- [35] J. Zhang, Y. Liu, L. Cui, S. Hao, D. Jiang, K.Y. Yu, S. Mao, Y. Ren, H. Yang, "Lattice Strain Matching"-Enabled Nanocomposite Design to Harness the Exceptional Mechanical Properties of Nanomaterials in Bulk Forms, *Adv. Mater.* 32 (2020) 1904387.
- [36] J. Zhang, Y. Liu, H. Yang, Y. Ren, L. Cui, D. Jiang, Z. Wu, F. Guo, S. Bakhtiari, Fotazedian, J. Li. Achieving 5.9% elastic strain in kilograms of metallic glasses: Nanoscopic strain engineering goes macro, *Mater. Today*. 37 (2020) 18-26.
- [37] X. Hu, Y. Liu, F. Guo, K. Yu, D. Jiang, Y. Ren, H. Yang, L. Cui, Enhanced superelasticity of nanocrystalline NiTi/NiTiNbFe laminar composite, *J. Alloy. Compd.* 853 (2021) 157309.
- [38] F. Motazedian, J. Zhang, Z. Wu, D. Jiang, S. Sarkar, M. Martyniuk, C. Yan, Y. Liu, H. Yang, Achieving ultra-large elastic strains in Nb thin films on NiTi phase-transforming substrate by the principle of lattice strain matching, *Mater. Des.* 197 (2021) 109257.
- [39] M.A. Meyers, Y.B. Xu, Q. Xue, M.T. Perez-prado, T.R. McNelly, Microstructural evolution in adiabatic shear localization in stainless steel, *Acta Mater.* 51 (2003) 1307-1325
- [40] G.D. Sim, Y. Hwangbo, H.H. Kim, S.B. Lee, J.J. Vlassak, Fatigue of polymer-supported Ag thin films, *Scripta Mater.* 66 (2012) 915-918.
- [41] V. Novak, P. Sittner, G.N. Dayanada, F.M. Braz-Fernandes, K.K. Mahesh, Electric resistance variation of NiTi shape memory alloy wires in thermomechanical tests: Experiments and simulation, *Mater. Sci. Eng. A* 481-482 (2008) 127-133
- [42] J. Zhang, S. Hao, D. Jiang, Y. Huan, L. Cui, Y. Liu, Y. Ren, H. Yang, Dual Phase Synergy Enabled Large Elastic Strains of Nanoinclusions in a Dislocation Slip Matrix Composite, *Nano Lett.* 18 (2018) 2976-2983
- [43] J.A. Shaw, S. Kyriakides, Thermomechanical aspects of NiTi, *J. Mech. Phys. Solids.* 43 (1995) 1243-1281.

- [44] M.L. Young, M.F.-X. Wagner, J. Frenzel, W.W. Schmahl, G. Eggeler, Phase volume fractions and strain measurements in an ultrafine-grained NiTi shape-memory alloy during tensile loading, *Acta Mater.* 58 (2010) 2344-2354.
- [45] G. Tan, Y. Liu, Comparative study of deformation-induced martensite stabilisation via martensite reorientation and stress-induced martensitic transformation in NiTi, *Intermetallics* 12 (2004) 373-381.
- [46] Y. Chen, O. Molnarova, O. Tyc, L. Kaderavek, L. Heller, P. Sittner, Recoverability of large strains and deformation twinning in martensite during tensile deformation of NiTi shape memory alloy polycrystals, *Acta Mater.* 180 (2019) 243-259.
- [47] M. Jin, A.M. Minor, E.A. Stach, J.W. Morris, Direct observation of deformation-induced grain growth during the nanoindentation of ultrafine-grained Al at room temperature, *Acta Mater.* 52 (2004) 5381-5387.
- [48] H. Hahn, P. Mondal, K.A. Padmanabhan, Plastic deformation of nanocrystalline materials, *NanoStruct Mater.* 9 (1997) 603-606.
- [49] J. Schiøtz, T. Vegge, F. Tolla, K.W. Jacobsen, Atomic-scale simulations of the mechanical deformation of nanocrystalline metals, *Phys. Rev. B* 60 (1999) 11971-11983.
- [50] C. Brandl, E. Bitzek, P.M. Derlet, H.V. Swygenhoven, Slip transfer through a general high angle grain boundary in nanocrystalline aluminum, *Appl. Phys. Lett.* 91 (2007) 111914.1-111914.3.
- [51] A.J. Haslam, D. Moldovan, V. Yamakov, D. Wolf, S.R. Phillpot, H. Gleiter, Stress-enhanced grain growth in a nanocrystalline material by molecular-dynamics simulation, *Acta Mater.* 51 (2003) 2097-2112.
- [52] D.S. Gianola, S. Van Petegem, M. Legros, S. Brandstetter, H. Van Swygenhoven, K.J. hemker, Stress-assisted discontinuous grain growth and its effect on the deformation behavior of nanocrystalline aluminum thin films, *Acta Mater.* 54 (2006) 2253-2263.
- [53] G.J. Fan, L.F. Fu, D.C. Qiao, H. Choo, P.K. Liaw, N.D. Browning, Grain growth in a bulk nanocrystalline Co alloy during tensile plastic deformation, *Scripta Mater.* 54 (2006) 2137-2141.
- [54] Y.J. Wei, C. Su, L. Anand, A computational study of the mechanical behavior of nanocrystalline fcc metals, *Acta Mater.* 54 (2006) 3177-3190.
- [55] F. Sansoz, J.F. Molinari, Incidence of atom shuffling on the shear and decohesion behavior of a symmetric tilt grain boundary in copper, *Scripta Mater.* 55 (2004) 1283-1288.
- [56] L. Ding, Y. Zhou, Y. Xu, P. Dang, X. Ding, J. Sun, Learning from superelasticity data to search for Ti-Ni alloys with large elastocaloric effect, *Acta Mater.* 218 (2021) 117200.
- [57] X. Zhu, X. Zhang, M. Qian, M. Imran, Elastocaloric effects related to B2 \leftrightarrow R and B2 \leftrightarrow B19' martensite transformations in nanocrystalline Ni_{50.5}Ti_{49.5} microwires, *J. Alloy. Compd.* 792 (2019) 780-788.

Comparison of cracking behavior of nanocrystalline Cu film on substrates of different plastic deformation mechanisms

G. Zhang ^a, T. Wang ^{a,b}, Z. Ma ^a, H. Zhou ^c, L. Cui ^a, K.Y. Yu ^{a*}

^a Department of Materials Science and Engineering, China University of Petroleum-Beijing, Beijing 102249, China

^b School of Materials Science and Engineering, Shaanxi University of Technology, Hanzhong, Shaanxi 723001, China

^c X-ray Science Division, Argonne National Laboratory, Lemont, IL 60439, USA

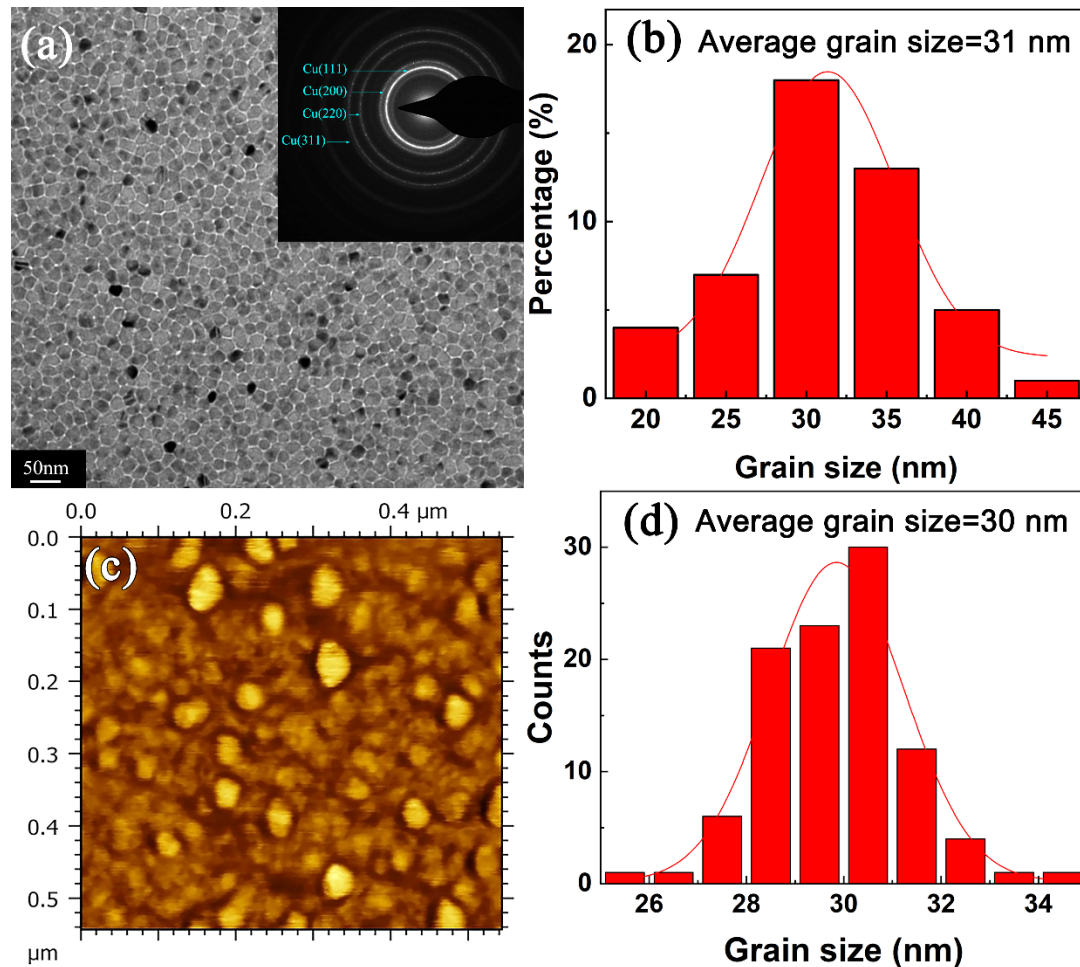


Fig. 1. (a) Plan-view bright-field TEM image of as-deposited nanocrystalline Cu films ($h=50$ nm) on carbon-coated TEM washer. Inset shows SAD pattern with indexed diffraction rings. (b) Grain size statistics based on TEM results, showing an average grain size of ~ 31 nm. (c) AFM image of the surface of as-deposited Cu films ($h=50$ nm) on NiTi substrate. (d) Grain size statistics based on AFM results, showing an average grain size of ~ 30 nm.

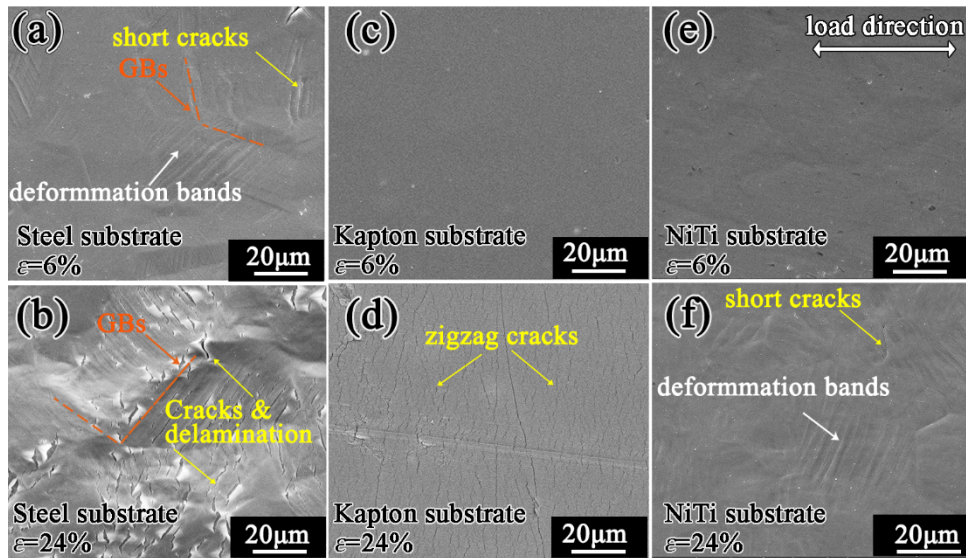


Fig.2. Crack evolution with increasing applied tensile strain (ϵ) in 50 nm Cu films on different substrates. (a) Steel substrate, $\epsilon=6\%$. (b) Steel substrate, $\epsilon=24\%$. (c) Kapton substrate, $\epsilon=6\%$. (d) Kapton substrate, $\epsilon=24\%$. (e) NiTi substrate, $\epsilon=6\%$. (f) NiTi substrate, $\epsilon=24\%$. Loading is along the horizontal direction.

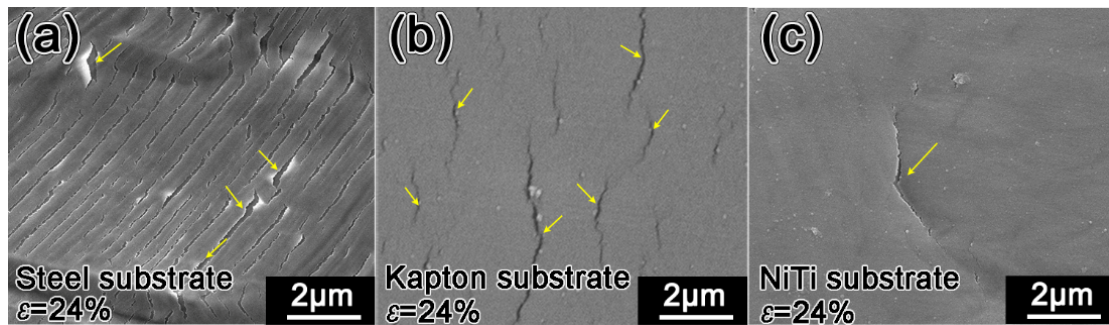


Fig. 3. Enlarged view of cracks in 50 nm Cu films at an applied strain of 24% on different substrates. (a) Steel substrate. (b) Kapton substrate. (c) NiTi substrate. Loading is along the horizontal direction.

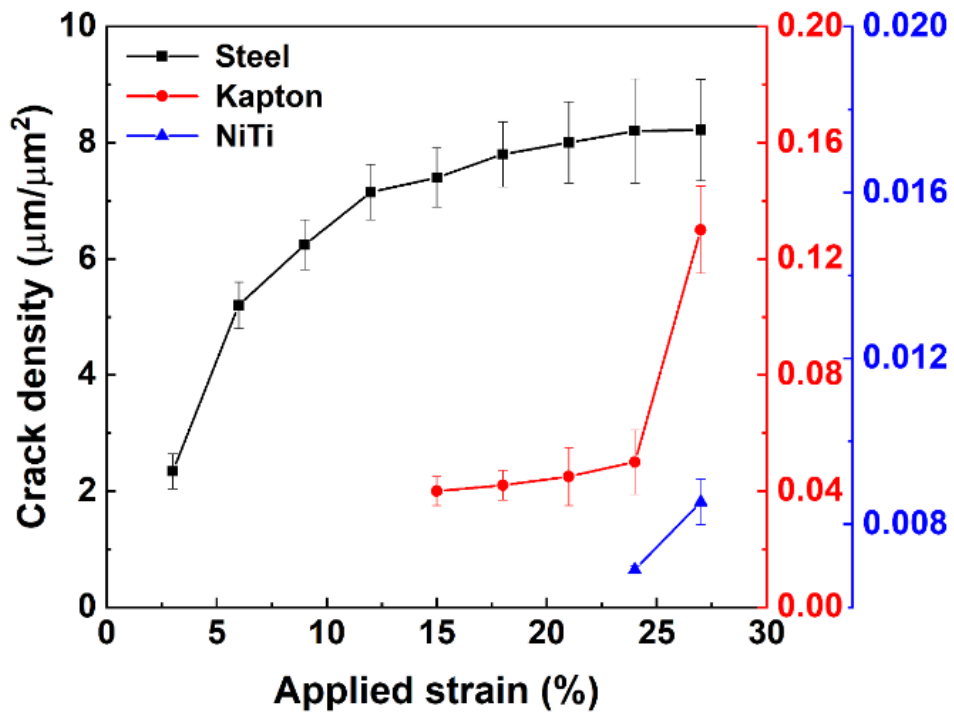


Fig. 4. Crack density as a function of applied strain for Cu films on different substrates. Crack density was denoted as the crack length per unit area.

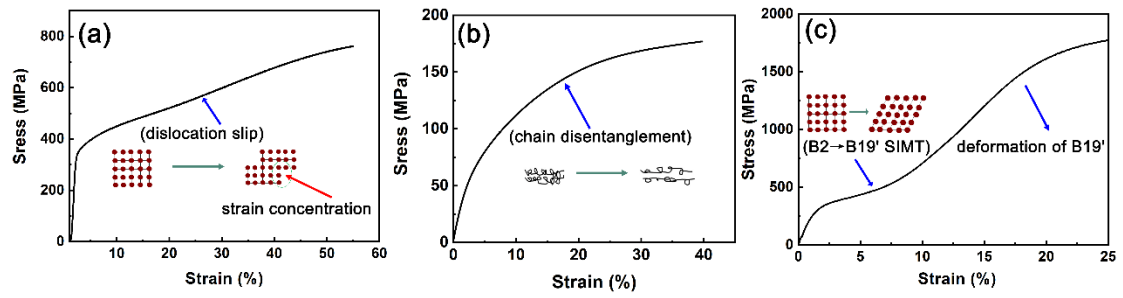


Fig. 5. Stress-strain curves of different substrates and the illustrated plastic deformation mechanisms. (a) Steel substrate. Plasticity occurs by dislocation slip. (b) Kapton substrate. Plasticity occurs by molecule chain disentanglement. (c) NiTi substrate. Plasticity occurs by stress-induced B2 \rightarrow B19' transformation and dislocation slip of B19' martensite.

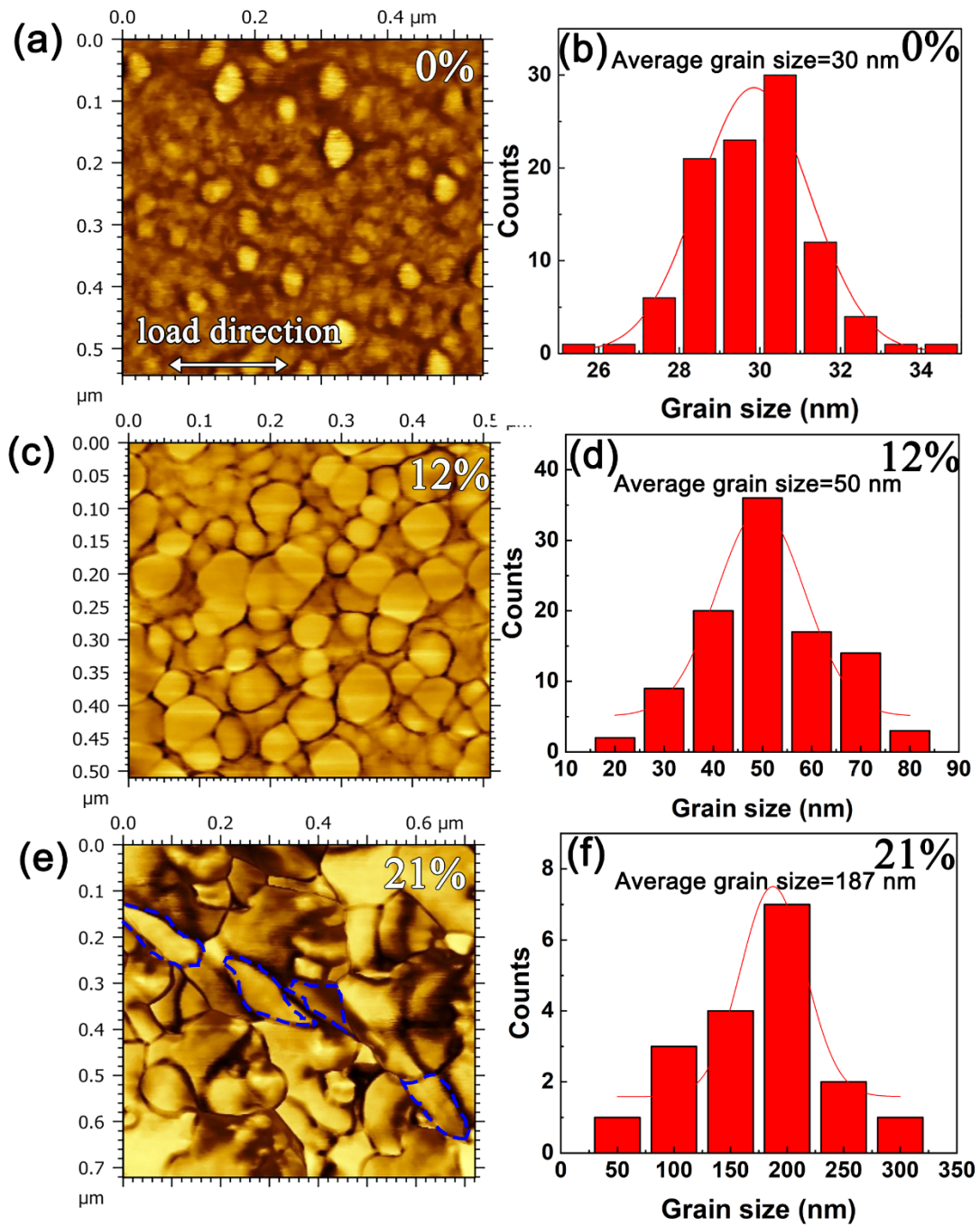


Fig. 6. (a, c, e) Grain morphology of Cu films on NiTi substrate at different applied strains observed by AFM. The outlines in e show the elongated grains. (b, d, f) Grain size statistics of Cu films at different applied strain.